MIXED-MODE FRACTURE TOUGHNESS OF ADVANCED CERAMICS

W. Brocks[1], F. Fischer[2], K.-F. Fischer[3], P. Gummert[4], E.Krämer[4], J. Mohn[4], P. Reimers[5], E. Rudolph[6], J. Thaten[4]

Three different specimen geometries with a relative notch depth of $a/W = 0.25$ of a well characterized silicon nitride used for high performance applications are tested under combined bending and torsion, i.e. mode I and mode III fracture. Much effort was made in designing, adjusting and calibrating the loading frame and rig in order to have defined and reproducable testing conditions. The crack faces were investigated fractographically by laser-optical methods for effects of increasing torsion. The objective of the tests is an experimental verification of mixed mode fracture criteria discussed in the literature.

INTRODUCTION

Some properties of ceramic materials make them increasingly interesting for advanced technological applications, i.e. their resistance to high temperatures and corrosion as well as their hardness and wear resistance. Hence, fields of practical application are found for chemical apparatus, combustion engines and turbines, and medical implants. But there are also a number of drawbacks resulting from the brittleness of these materials, their inability to reduce stress concentrations by plastic deformations and the usually large scatter of their strength properties. Reliable assessments of durability and service life time require an established characterization of strength and toughness properties and verified fracture criteria.

Fracture in brittle materials occurs under linear elastic deformations. Linear

1 Fraunhofer Institut für Werkstoffmechanik, Freiburg
2 Bergakademie Freiberg
3 Hochschule für Wirtschaft und Technik, Zwickau
4 Technische Universität Berlin
5 IWiS GmbH, Berlin
6 Bundesanstalt für Materialforschung und -prüfung, Berlin

elastic fracture mechanics (LEFM) of metals under mode I loading conditions is a well founded concept of failure assessment, and the determination of fracture toughness, K_{Ic} , is layed down in testing standards, e.g. (1). Though the basic theory is the same, comparably established concepts do not exist for ceramic materials, and a straightforward transfer of specimen fabrication and testing conditions from metals to ceramics is not possible. Size and geometry effects are still under discussion (2). Much more open questions concern the fracture behaviour under mixed mode conditions. But just this kind of loading is of high practical relevance for a realistic failure assessment, especially the case of combined bending and torsion, i.e. mode I and mode III. This statement holds in general with respect to verified mixed mode fracture criteria (3) and, of course, especially for ceramics. The investigations which are reported here intend to contribute to the experimental verification of fracture criteria for ceramic materials under mixed mode. Three different specimen geometries were tested under varying ratios, M_b/M_t , of bending moment and torque. Stress intensity factors, K_I , K_{III} , were determined from handbook solutions and numerical analyses.

EXPERIMENTS

All tests were performed at room temperature with individually produced specimen of one stock of sintered silicon nitride. The electron microscopy of a polished four point bend specimen showed round and band shaped inclusions (0.6-0.7 % Al, 0.1-0.2 % Fe, 2.5-3.5 % La) at the specimen surface and at the nuclei of main and side cracks of the crack face, Fig. 1. The mechanical properties which are summarized in Table 1 were determined according to the respective standards. The four point bend (4PB) strength of 29 specimens was between 723 and 953 *MPa*. The estimates of the Weibull parameters as determined by the method of maximum likelihood were $\hat{m}$ = 30.8 and $\hat{\sigma}_u$ = 913 *MPa*. A fracture toughness of K_{Ic} = 7.4±0.2 $MPa\sqrt{m}$ was measured from standard 4PB specimens with a machined slit of a/W = 0.252±0.007 at an average loading rate of 41 *N/s*. It is used as a reference value for the fracture tests under combined bending and torsion.

Three different specimen geometries, i.e. a round bar with circumferential notch (RU), a round bar with single edge notch (RS), and a rectangular bar with single edge notch (RE), but the same relative notch depth of a/W = 0.25, see Table 2, have been tested. The rectangular bars were manufactured according to the specifications of the German standard drafts DIN (E) 51110, part I, and DIN (E) 51109. All round bars were supplied round polished with a tolerance in diameter of ±0.05 *mm*. They were cemented in guide sleeves before machining the slit and for centering them in the text fixture. The notch root widths lay between 80 and 100 µ*m*.

The strength tests were performed with a standard 4PB bending fixture in

a displacement controlled testing machine. A special test fixture was designed for the mixed mode tests, Fig. 2, which was installed in a loading frame with hydraulic cylinder and run load controlled. Varying ratios of bending to torsional moment, M_b/M_t , were realized by keeping the load span, b, for 4PB constant whereas the lever arm, c, for applying the torque was varied, see Table 3. The supports and the load pins of the mixed mode test fixture allow for rotation of the specimen around its axis but are axially fixed. This kind of test condition is different from the standard 4PB test fixture where roller pins are used to minimize friction. Friction effects may hence occur in the mixed mode test fixture and yield higher fracture loads and, thus, increased K_c-values.

The test fixture was checked by testing steel specimens with several strain gauges applied along the specimen length and by finite element (FE) calculations. A maximum variation of strains of ±2 μm was measured within the range of constant bending moment, i.e. between the span of the applied loads, and the FE studies showed that a variation of the load span, b, between 20 and 40 mm had no influence on the stresses in the cracked section. A FE analysis of the round bar with circumferential notch confirmed that no crack closure will occur in the compression zone under bending before fracture.

The specimens were tested up to fracture under pure bending, pure torsion and combined bending and torsion, see Table 4. Some examples of load vs. time curves are shown in Fig. 3. The loading rate was 41 N/s. Notch opening displacement was measured by a strain gauge applied over the notch. A constant increase of notch opening with the applied load indicated linear elastic behaviour, and no indication of sub-critical crack growth were observed.

CALCULATION OF STRESS INTENSITY FACTORS

Stress intensity factors for bending and torsion follow from

$$K_I = \sigma\sqrt{\pi a}\; Y_b\left(\frac{a}{W}\right) \quad ; \quad K_{III} = \tau\sqrt{\pi a}\; Y_t\left(\frac{a}{W}\right) \qquad (1).$$

Geometry functions for bending, Y_b , can be found for all the three specimen types in references (4), (5) and (6), and a K_{III}-solution for torsion of the circumferentially cracked round bar is given in (6). Whereas these solutions refer only to the maximum value, three-dimensional FE analyses also allow the determination of the variation of stress intensity along the crack front. Two different methods of calculating K have been used here, i.e. from the energy release rate (J-method), and from the displacements at the crack tip (u-method), references (7) and (8).

Fig. 4 shows the FE model of the RS specimen in its deformed configuration under pure bending with iso-lines of bending stresses. The homogenous stress distribution in the range of constant bending moment apart from the flawed section and the stress concentration at the crack front are evident. Examples for results of the *u*-method are shown in Fig. 5 for the RU specimen. For comparison, the handbook solution (6) is $K_{III} = 5.16\ MPa\sqrt{m}$ and the FE result $K_{III} = 5.11\ MPa\sqrt{m}$ for a torque of 100 *Nmm*. K_{III} is constant along the crack front, and K_I and K_{II} vanish for pure torsion. For pure bending, K_I varies with a cosine along the crack front due to the linear distribution of applied stresses with the *z*-coordinate. A comparison of geometry functions for bending, Y_b, determined numerically by the *J*-method with handbook solutions for all three specimen types is given in Fig. 6. If a 3D analysis is performed two limiting values are obtained from *J*, assuming either plane strain or plane stress conditions.

RESULTS

The standard 4PB bending test for determining fracture toughness gave a K_{Ic} value of 7.4±0.2 $MPa\sqrt{m}$ whereas a value of 7.7±0.2 $MPa\sqrt{m}$ was obtained with the mixed mode test fixture under pure bending. The difference of about 4% is probably due to friction effects as mentioned above.The results of the combined bending and torsion tests of the RU specimen are plotted in an interaction diagram where both axes are normalized by K_{Ic}, Fig.7. The evaluation of the test data of the two other specimen types is in progress. Hence only a few basic remarks (9) concerning the mixed mode fracture criterion can be made.

The criterion of total energy release rate results in a limiting curve

$$\left(\frac{K_I^c}{K_{Ic}}\right)^2 + \frac{4}{\kappa+1}\left(\frac{K_{III}^c}{K_{Ic}}\right)^2 = 1 \qquad (2)$$

with

$$\kappa = \begin{cases} 3-4\nu & \text{for plane strain} \\ \dfrac{3-\nu}{1+\nu} & \text{for plane stress} \end{cases} \qquad (3)$$

This criterion bases on the assumption that the crack extends in the ligament plane, i.e. its inclination angle is $\varphi_c = 0$. It also implies that

$$\frac{K_{Ic}}{K_{IIIc}} = \sqrt{\frac{4}{\kappa+1}} = \begin{cases} 1.19 & \text{for plane strain} \\ 1.14 & \text{for plane stress} \end{cases} \qquad (4)$$

which is not confirmed by the experiments where $K_{IIIc} = 12.7 \pm 0.7\ MPa\sqrt{m}$ and $K_{Ic} / K_{IIIc} = 0.58$. The mode III fracture toughness, K_{IIIc}, may be introduced as an additional parameter to obtain a more realistic mixed mode criterion.

The experimental data can be expressed within an error of 3,5% by the interaction curve

$$\left(\frac{K_I^c}{K_{Ic}}\right) + \left(\frac{K_{III}^c}{K_{IIIc}}\right)^{2.41} = 1 \qquad (5)$$

which is also plotted in Fig. 7.

As the inclination angle, φ_c, of the cracks are of basic importance for setting up a fracture criterion they are presently evaluated for all cracked specimens by a laser based roughness measuring technique. The shape of the fracture surface under pure torsion is schematically shown in Fig. 8. The crack starts from some point at the crack front at an angle of approximately 45°. In practice, it may extend in a more complicated way resulting in several cracked pieces if initiation occurs at several points simultaneously. Under superimposed bending, the cracks start at the tension side.

REFERENCES

(1) American Society for Testing and Materials: Standard test method for plane-strain fracture toughness of metallic materials, ASTM E 399, 1981.

(2) Shannon, J.L. and Munz, D., Specimen size and geometry effects on fracture toughness of aluminium oxide measured with short-rod and short-bar Chevron-notched specimens, ASTM STP 855, 1984, pp. 270-280.

(3) Fischer, K.-F., "Theoretical and Applied Fracture Mechanics", Vol. 1, 1984, pp. 117-131.

(4) Srawley, J.E. and Gross, B., "Cracks and Fracture", ASTM STP 601, American Society for Testing and Materials, 1976, pp. 559-579.

(5) Murakami, Y., "Stress Intensity Factors Handbook", Vol. 1 and 2, Pergamon Press, Oxford, 1987.

(6) Theilig, H. and Nickel, J., "Spannungsintensitätsfaktoren", VEB Fachbuchverlag, Leipzig, 1987.

(7) Ingraffea, A.R. and Manu, C., Int. J. Num. Meth. Engng., Vol. 15, 1980, pp.1427-1445.

(8) Chen, L.S. and Kuang, J.H., Engineering Fracture Mechanics, Vol. 45, 1993, pp. 21-23.

(9) Fischer, K.-F., Theor. and Appl. Fract. Mech. Vol. 3, 1985, pp. 85-95.

TABLE 1 - Sintered Silicon Nitride (SSN): Characterization of Material.

Elastic Constants:	Resonance Test following	
E [GPa]	ASTM C 848-88;	303.6
G [GPa]	3 Specimen	117.9
ν [-]		0.29
Geometric Bulk Density:	pr EN 623-2;	
ρ [Mg/m^3]	3 Specimen	3.25
Four Point Bend Strength:	DIN (E) 51110, Pt. 1 and 3;	
$\bar{\sigma}_{4B} \pm s_{n-1}$ [MPa]	29 Specimen	897 ±43
$\hat{\sigma}_o$ [MPa]		913
$\hat{m}_{Korr}$ [-]		30.8
90 % Confidence Intervals:		
σ_o [MPa]		$903 \leq \sigma_o \leq 923$
m [-]		$24 \leq m \leq 40$
Fracture Toughness:	DIN (E) 51 109;	
$\bar{K}_{Ic} \pm s_{n-1}$ [$MPa\sqrt{m}$]	8 Single Edge Notched Bend	7.4 ± 0.2
$\bar{\dot{K}} \pm s_{n-1}$ [$MPa\sqrt{m}\,s^{-1}$]	Beams (With a Notch Root	1.6 ± 0.04
$a/W \pm s_{n-1}$ [-]	Width of ca. 89 µm ;	0.254 ± 0.008
$\bar{F} \pm s_{n-1}$ [Ns^{-1}]	a/W = 0.25)	40.6 ± 0.09
t_v [s]		4.6

TABLE 2 - Specimen: Dimensions and Tolerances.

Geometry	Dimensions of Specimen		Description of Specimen
RE	Width [mm]	4.01 ... 4.05	Single Edge Notched Rectangular Beam (a = 1 mm,
	Thickness [mm]	2.99 ... 3.07	W = 4 mm) Used in Mixed Mode, Bending and Torsional
	Planparall. [mm]	0.01 ... 0.03	Loading
RS	Diameter [mm]	5.98 ... 6.01	Single Edge Notched Round Bar (a = 1.5 mm, D = 6mm)
	Notch Depth [mm]	1.49 ± 0.18	Used in Mixed Mode, Bending and Torsional Loading
RU	Diameter [mm]	5.98 ... 6.01	Circumferentially Notched Round Bar (a/2 = 0.75mm, D =
	Notch Depth [mm]	0.75 ± 0.19	6mm) Used in Mixed Mode, Bending and Torsional Loading

TABLE 3 - Adjustment of Bending/Torsional Fixture for different M_b/M_t-Ratios.

Nominal Moment Ratios	Nominal Edge Stress Ratios		Lower Span L and Upper Span b		Lever Arm
$M_{b(max)}/M_t$	$\sigma_{(max)}/\tau_{(max)}$ ● $\sigma_{(max)}/\tau_{(max)}$ ▌		L [mm]	b [mm]	c [mm]
0	0	0	70		60
0.25	0.5	0.269	70	40	60
0.5	1.0	0.539	70	40	30
1.0	2.0	1.077	70	40	15
2.0	4.0	2.154	70	40	7.5
∞	∞	∞	70	40	0

TABLE 4 - Mixed Mode Fracture Tests: Mean and Standard Deviation of Peak Loads for Different Test Geometries with Increasing M_b/M_t-Ratios.

M_b/M_t	0	0.25	0.5	1.0	2.0	∞
Geometry	Peak Load [N]					
RE	52.2 ±1.9	42.1 ± 1.5	70.4 ± 1.9	105.7 ± 4.0	121.2 ± 4.4	137.2 ± 4.8
RS	200.4 ± 8.2	161.0 ± 5.0	278.0 ± 23.8	350.9 ± 12.1	390.5 ± 5.7	371.4 ± 4.0
RU	266.3 ± 10.4	183.9 ± 7.6	274.0 ± 8.2	339.7 ± 13.2	345.8 ± 24.3	346.8 ± 9.2

Figure 1. Four Point Bend Specimen with σ_{4B} = 723 N/mm^2 : Large Inclusion at the Tensile Surface with Mean and Side Cracks.

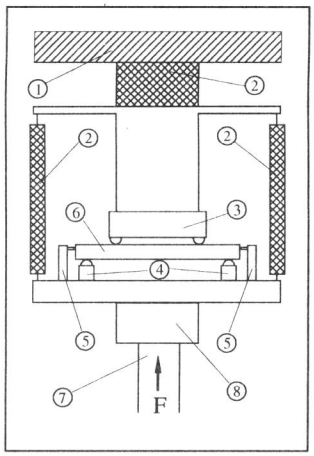

Figure 2. Arrangement of the Mixed Mode Test Fixture.

1) frame
2) 1 kN - load cell used in load control
3) fixed-contact flexure loading member
4) fixed-contact supports for torsional lever arms
5) vertical specimen guide
6) specimen
7) hydraulic stamp
8) 1 kN-load cell used as measuring device

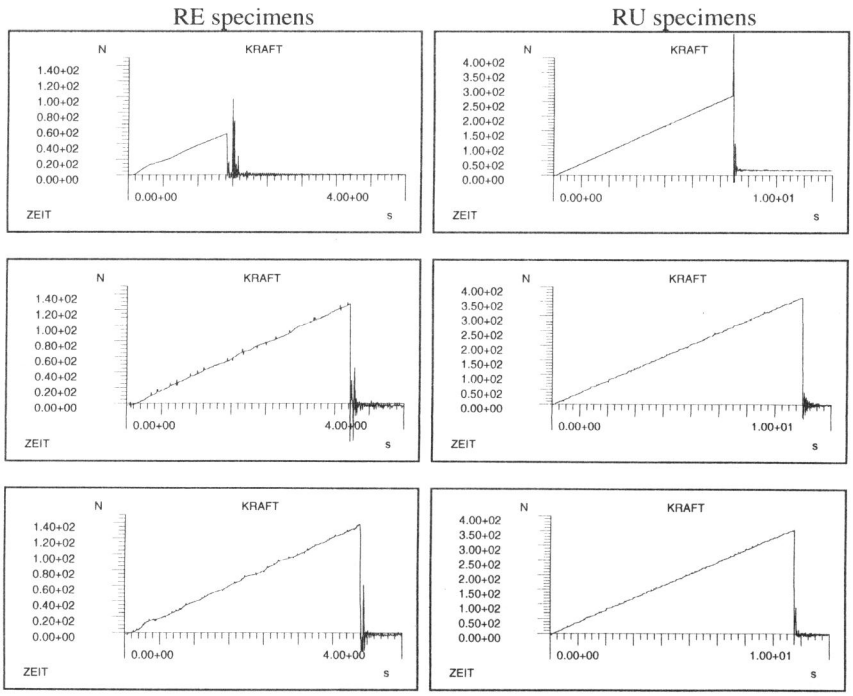

Figure 3. Original Force-vs.-Time-Plots of some RE and RU Specimens at M_b / M_t Ratios of 0, 2.0, ∞ (from above).

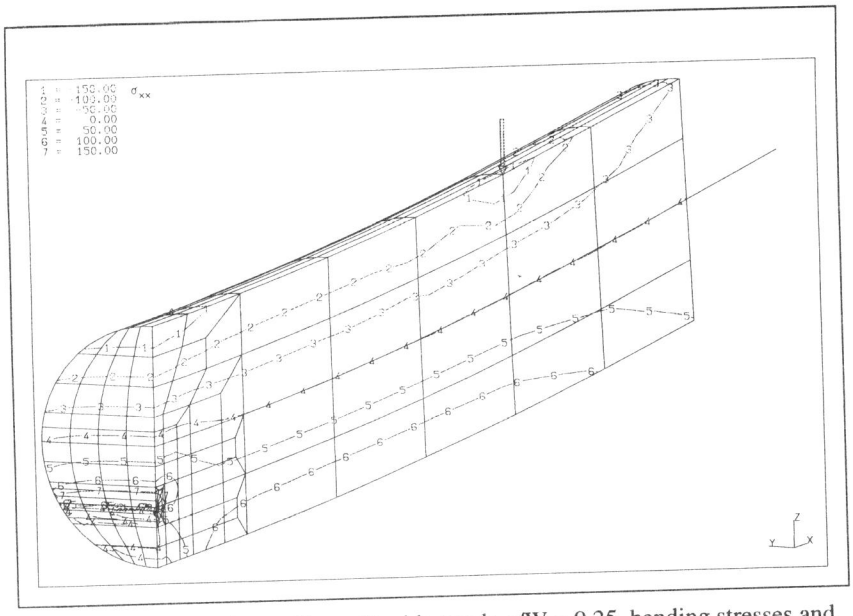

Figure 4. FEM-model round bar with side notch, a/W = 0.25, bending stresses and displacements.

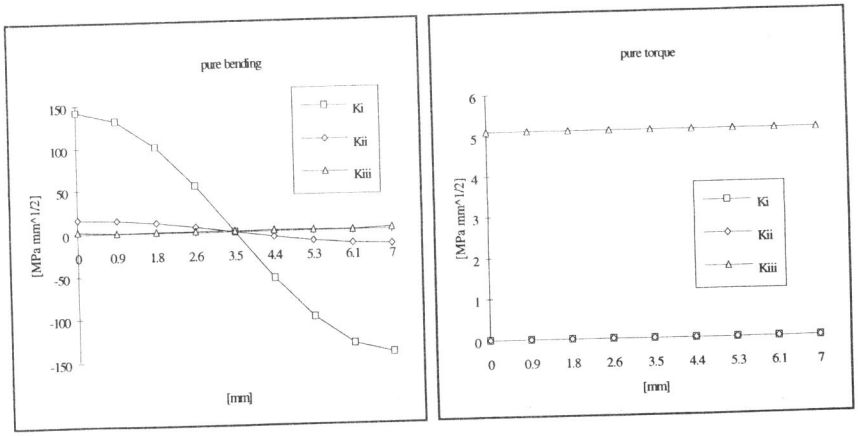

Figure 5. SIF curves along half part of crack front, round bar with circumferential notch, u-method.

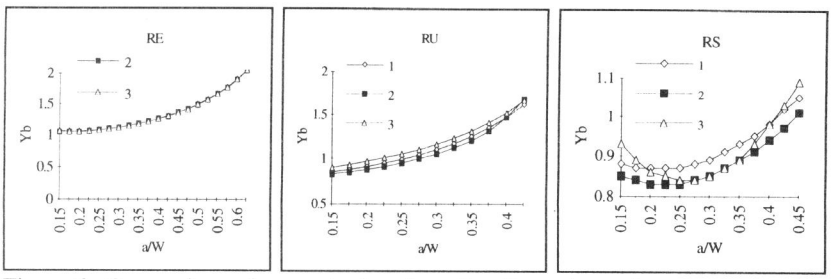

Figure 6. Comparison of geometry functions for all specimen shapes, pure bending; 1: FEM plane strain, 2: FEM plane stress, 3: Handbook solutions

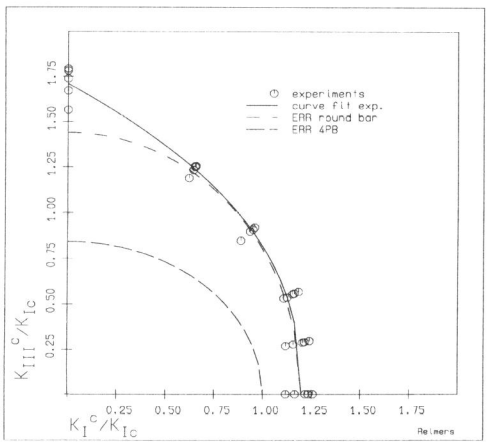

Figure 7. Mixed mode interaction diagram:
experiments on round bar with circumferential notch;
curve fit experiments eq. (5),
ERR = energy release rate criterion, eq. (2),
K_{Ic} from 4PB or round bar specimens, respectively

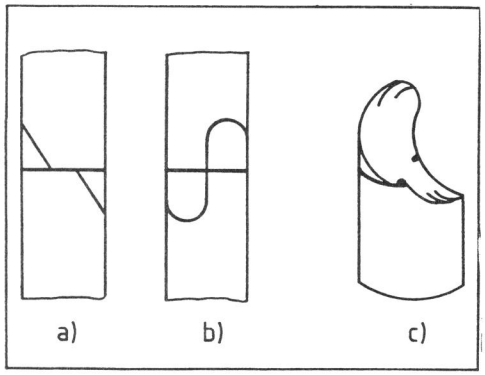

Figure 8. Round bar with circumferential notch under pure torsion,
shape of fracture surface:
(a) frontview,
(b) backview,
(c) perspective view with crack initiation point